Hindawi
Journal of Sensors
Volume 2023, Article ID 6807212, 13 pages
https://doi.org/10.1155/2023/6807212

Research Article

New Foundation Treatment Technology Using Cement Soil Composite Tubular Piles Supported by Optical Fiber Sensing Technology

Fan Sun

College of Civil Engineering and Architecture, Zhejiang University, Hangzhou, 310058 Zhejiang, China

Correspondence should be addressed to Fan Sun; 11512027@zju.edu.cn

Received 18 July 2022; Revised 19 September 2022; Accepted 29 September 2022; Published 8 May 2023

Academic Editor: Linesh Raja

The purpose is to optimize the foundation's treatment process and improve the foundation's construction effect to better apply the cement soil composite tubular piles. This exploration is to study the cement composite tubular piles. First, the principle and application of optical fiber sensing technology are discussed. Then, the application design and conditions of the cement composite tubular pile are discussed. Finally, a new foundation treatment technology supported by optical fiber sensing technology is proposed and comprehensively evaluated based on the application of cement soil composite tubular piles. The research results show that: (1) the new foundation treatment technology reflects the optimization of the optical fiber sensing technology for the foundation treatment. Moreover, it is further optimized through the application of cement soil composite tubular piles. (2) When subjected to the same load, the longer the core pile is, the smaller the cement soil composite pile's settlement is. When the inner core pile is 20 m ~24 m long, the settlement of the cement soil composite pile is small. When the length of the inner core pipe pile is 16 m ~20 m, the settlement range of cement soil composite pile becomes larger. (3) With the increase of friction coefficient, the settlement distance of cement soil composite tubular pile will decrease. The above data show that compared with the traditional foundation treatment technology, the new foundation treatment technology designed based on the application of composite tubular piles, supported by optical fiber sensing technology, can well solve the foundation construction problems, avoid pavement settlement, cracking, and other phenomena, and ensure the overall safety of the road. This exploration fully reflects the advantages of the new technology of foundation treatment and ensures the quality of road engineering. It provides a reference for the development of foundation treatment technology of construction projects and contributes to the development of the construction industry.

1. Introduction

Currently, the scale of infrastructure construction in China is increasingly large, super large, super heavy, and super high-rise buildings are springing up on the land of the motherland. Buildings have higher and higher requirements for the foundation's bearing capacity and deformation control. However, most of the underground soil layers of sites that can be adopted for construction in cities are complex, and construction teams need to carry out construction on complex soil layers with large changes in stiffness and flexibility [1]. Hence, in modern project engineering, the speculative proportion of foundation and the engineering quantity of foundation construction are considerable and are increasingly higher. The quality of the foundation can even determine the construction quality of buildings [2]. Accidents that cause dangerous situations in buildings due to problems in the foundation occur frequently. The foundation is a hidden project. Once a problem arises, the personnel, materials, and funds to repair the foundation are huge. With the increasing development of the construction industry, in addition to providing sufficient safety, the current construction scheme also needs to be highly economical and have a short construction period. In this way, the construction party can construct to serve society as soon as possible [3]. Since entering the 21st century, the domestic economy has

entered a period of rapid development. High-rise, super high-rise buildings, and heavy structures have been continuously built, and pile foundation projects have also been developed rapidly. Various new pile types, processes, and technologies are emerging, and some new fields have emerged, showing a new development trend. Pile foundations are developing towards large-diameter long piles, micro piles, high-strength piles, and composite piles. Given the development direction of pile foundation, combined with the characteristics of the east coast of China and the alluvial plain strata of rivers and lakes, Shandong Academy of Building Sciences has developed a composite pile technology, namely cement soil composite tubular pile technology, which is suitable for soft soil areas. The cement soil composite tubular pile is composed of the cement soil pile formed by the high-pressure jet mixing method and the concentrically implanted prestressed high-strength concrete tubular pile. It has the characteristics of large diameter, long pile, high bearing capacity, high-cost performance, and high construction efficiency. As a new technology, the bearing mechanism of cement soil composite tubular pile is obviously different from that of an ordinary pile, and the mechanical performance of the composite pile is also greatly different from that of the existing core inserted pile technology. In order to make the resistance of the soil around the pile and the strength of the pile material reach the limit state at the same time, meet the theoretical optimal matching relationship, and give full play to the technical advantages of the cement soil composite tubular pile, it is essential to research the bearing mechanism of the cement soil composite tubular pile. Based on the field test and numerical simulation test, this exploration studies the vertical compressive bearing mechanism of cement soil composite tubular pile, and obtains the influence rules of cement soil pile diameter, tubular pile diameter, cement soil pile length, tubular pile length, cement soil strength, stratum conditions, and other factors on the vertical compressive bearing mechanism of cement soil composite tubular pile.

Recently, the rising optical fiber sensing technology has attracted more and more researchers' attention. The characteristics such as durability, small volume, strong anti-electromagnetic interference ability, and portability make the optical cable easy to lay and install, good matching with the measurement target, and small stress impact on the measured target. It can carry out signal transmission. Good use of optical fiber sensing technology can realize real-time, remote and all-weather measurements of various structures in civil engineering [4]. The distributed optical fiber sensing technology based on Brillouin Optical Time Domain Reflectometry (BOTDR) has the characteristics of long monitoring distance, fast signal transmission, and high accuracy. According to these characteristics, it can be adopted for remote real-time monitoring of each item in the project to ensure its smooth progress [5]. In some developed countries, the application of optical fiber in civil engineering has been studied for decades. For example, Japan, Switzerland, France, and the United States have made crucial inventions and innovations in this technology. These studies have laid a good foundation for future projects' health monitoring and safety early warning [6]. The common distributed optical fiber sensing technology can be divided into the following two categories: interferometric distributed optical fiber sensing technology and scattering distributed optical fiber sensing technology. Among them, the distributed optical fiber sensing technology based on the interference principle appears earlier. It includes the distributed optical fiber sensing technology based on Michelson optical fiber interferometer, based on Mach-Zehnder optical fiber interferometer, based on Sagnac optical fiber interferometer, and based on composite structure interferometer. Distributed optical fiber sensing technology based on the scattering principle appears late, including distributed optical fiber sensing technology based on Raman scattering, distributed optical fiber sensing technology based on Brillouin scattering and distributed optical fiber sensing technology based on Rayleigh scattering.

A new foundation treatment technology supported by optical fiber sensing technology is proposed. It is to use optical fiber sensing technology to realize automatic monitoring of foundation settlement. Then, the stress characteristics and working mechanism of cement soil composite tubular piles are studied. The influence of the bearing capacity of cement soil composite tubular piles on settlement is researched. Next, the deformation and settlement law of the foundation based on cement soil composite tubular piles are obtained to study the reasonable method of foundation treatment and reduce the uneven settlement of the pavement and pavement damage. This exploration provides a reference for the development of foundation treatment technology of construction engineering and contributes to the development of the construction industry.

2. Methods

2.1. Optical Fiber Sensing Technology. Distributed optical fiber sensing technology based on Optical Time Domain Reflection (OTDR) includes Rayleigh OTDR and BOTDR [7]. The advantage of distributed optical fiber sensing technology is that it can simultaneously measure the continuously distributed temporal and spatial information on the optical fiber path without making multiple-point sensors. It overcomes the defect that the traditional point sensor is difficult to monitor the measured object continuously in an all-round way. Moreover, it has good performance that traditional sensors do not have, such as less energy loss and data transmission of multiple signals [8]. OTDR measurement technology is to receive the pulse signal of light in the optical fiber, and then transmit the pulse signal of light in the optical fiber. When the pulse signal of light encounters the nature of the optical fiber itself, the interface, the bending of the optical fiber, the optical fiber connecting other devices, or other similar events, the pulse signal of light will produce reflected light and scattered light. Part of the reflected light and scattered light will return to the pulse signal port of the emitted light along the same path [9]. According to the time difference t between the pulse signal of the emitted light and the pulse signal of the received light, OTDR can

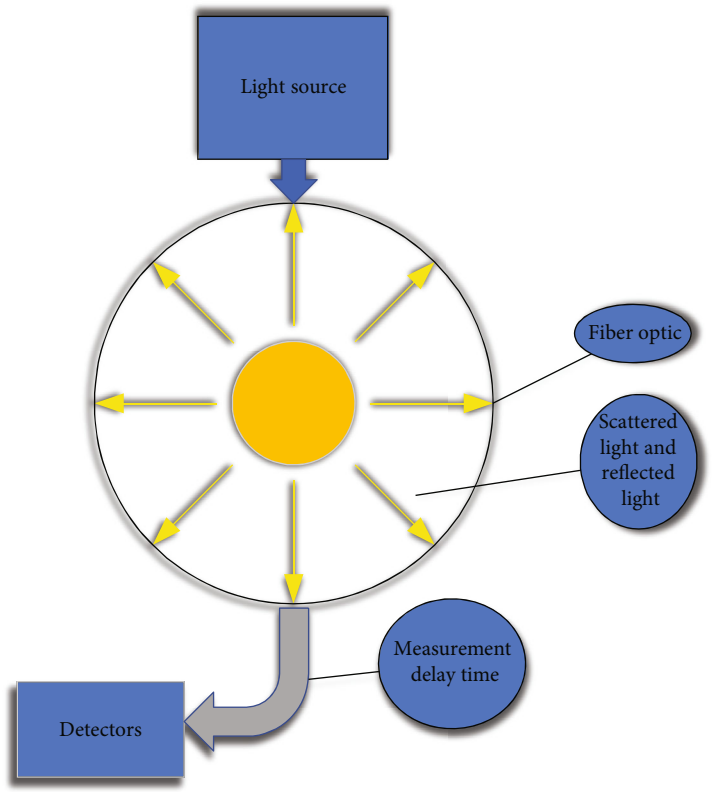

Figure 1: The schematic diagram of OTDR technology.

calculate the distance d between the above measurement point and OTDR through:

$$d = \frac{ct}{2n}. \quad (1)$$

c is the propagation speed of light in the optical fiber; n is the refractive index of the optical fiber itself [10].

Figure 1 displays the principle of OTDR technology.

OTDR technology can continuously display the loss distance of optical pulse and the changes of scattered light and refracted light on the whole optical fiber line, without any damage to the optical fiber during measurement.

Optical fiber sensing technology is widely adopted in structural engineering detection. For example, reinforced concrete is a widely used material at present. Embedding optical fiber materials directly in concrete structures or pasting them on the surface is the main application form of optical fiber, which can detect thermal stress and curing, deflection, bending, stress, and strain. The concrete will generate a temperature gradient due to hydration during solidification. If the cooling process is uneven, the thermal stress will cause cracks in the structure. The use of optical fiber sensors embedded in concrete can monitor its internal temperature changes, thus controlling the cooling rate. Hence, the optical fiber sensing technology will have a significant application prospect in the foundation treatment.

2.2. Fiber and Brillouin Scattering. The silicon material of optical fiber is a kind of electrostrictive material. When the high-power pump light propagates in the fiber, its refractive index will increase, resulting in the electrostriction effect, which causes most of the transmitted light to be converted into the backscattered light, resulting in stimulated Brillouin scattering. The specific process is as follows: when the pump light propagates in the optical fiber, its self-issued Brillouin scattering light propagates in the opposite direction of the pump light. When the intensity of the pump light increases, the intensity of the self-issued Brillouin scattering increases. When it increases to a certain extent, the backward transmitted Stokes light and the pump light will interfere, producing strong interference fringes, which greatly increases the local refractive index of the fiber. In this way, a sound wave will be generated due to the electrostriction effect. The sound wave generation will stimulate more Brillouin scattering light, and the generated scattering light will strengthen the sound wave. Such interaction produces strong scattering, which is called stimulated Brillouin scattering. Compared with light waves, the energy of sound waves is negligible. Hence, without considering the acoustic wave, the process of stimulated Brillouin scattering can be summarized as the process of energy transfer from higher frequency pump light to lower frequency Stokes light. In this way, stimulated Brillouin scattering can be regarded as a process of optical gain for Stokes light propagating in electrostrictive materials in the presence of pump light. In stimulated Brillouin scattering, although the anti-Stokes and Stokes light exist theoretically, they are generally only Stokes light.

2.3. Basic Principles of BOTDR. BOTDR is a technology that uses the relationship between Brillouin scattering frequency

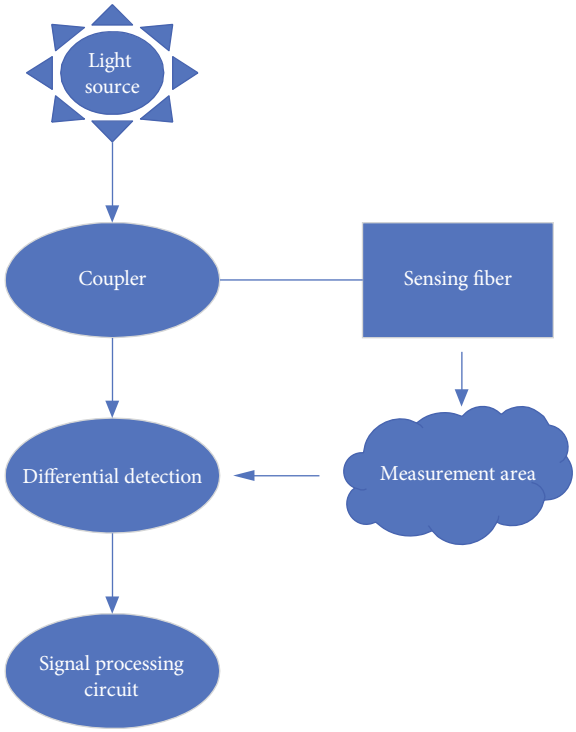

Figure 2: Basic block diagram of distributed optical fiber sensing system based on BOTDR.

shift in optical fiber, the temperature of optical fiber and the strain of optical fiber to realize measurement [11]. The distributed optical fiber sensor based on BOTDR is a measurement sensor for stress change and temperature change combined with OTDR measurement technology and Brillouin scattering. Figure 2 presents the principle:

The detector receives Brillouin scattering light, which will have a frequency shift relative to the pulse signal of the incident light [12]. When the temperature of the optical fiber changes and strains occur, the refractive index n of the optical fiber core and the propagation speed v of light in the optical fiber will change accordingly, resulting in the change of Brillouin frequency shift [13]. Since Brillouin frequency shifts are linearly related to fiber temperature and strain, it is only necessary to measure the change of Brillouin frequency shift to obtain the change of temperature and generated stress and strain. Measuring the return time of scattered light can determine the position of the corresponding point.

In fact, in the distributed optical fiber sensor system based on BOTDR, the output continuous light of the laser is modulated into pulse light and shoots into the sensing fiber to generate Brillouin Stokes and anti-Stokes light with frequency shifts up and down. A filter is adopted to filter out the scattered light signal of one of the frequencies detected by the photodetector. Through signal processing, the Brillouin gain spectra at different positions are fitted by Lorentz to obtain the Brillouin frequency shift curve along the fiber. According to the corresponding relationship between Brillouin frequency shift and temperature and stress, the change of external temperature and stress can be deduced. BOTDR technology can realize both distributed temperature sensing and stress sensing. However, due to the limited incident light power of BOTDR, the natural attenuation of optical fiber makes the sensing signal weak and difficult to detect, and shortens sensing distance.

Figures 3 and 4 show the relationship between the frequency shift change of Brillouin scattered light and strain and temperature in BOTDR measurement technology:

Figures 3 and 4 reveal that if the temperature change of the working environment where the optical fiber is located is less than 4°C, the influence of temperature on Brillouin frequency shift is ignored. When the stress change of the optical fiber is 0, the change of temperature is positively and linearly related to the change of Brillouin frequency shift, that is:

$$\nu_B(T) = \nu_B(T_0) + \frac{d\nu_B(T)}{dT}\Delta T. \tag{2}$$

T_0 is the initial temperature, T is the temperature at the time of measurement, and $\triangle T$ is the temperature change [14].

Moreover, Figure 3 shows that the relationship between Brillouin frequency shift and fiber temperature and fiber strain is [15]:

$$\nu_B(\varepsilon, T) = \nu_B(0, T_0) + \frac{\partial \nu_B(\varepsilon, T)}{\partial \varepsilon} + \frac{\partial \nu_B(\varepsilon, T)}{\partial T}. \tag{3}$$

$\nu_B(\varepsilon, T)$ is the Brillouin frequency shift change when the fiber strain is ε and the temperature is T. $\nu_B(0, T)$ is the Brillouin frequency shift when the fiber strain is 0 and the temperature is T_0. T_0 is the initial temperature, and T is the temperature at the measurement time. ε is strain. $\partial \nu_B(\varepsilon, T)/\partial \varepsilon$ is the relevant variation parameter between Brillouin frequency shift and strain, about 493 MHz. $\partial \nu_B(\varepsilon, T)/\partial T$ is the variation parameter between Brillouin frequency shift and temperature. The variation parameters between fiber temperature and fiber strain are compared. It is found that the stress change of light has a greater influence on the Brillouin frequency shift of light.

2.4. Structural Characteristics of Cement Soil Composite Tubular Piles. The cement soil composite tubular pile is composed of a core pile and a cement soil mixing pile. The prestressed high-strength tubular pile, cast-in-place pile, and structural steel are mainly used as the stiffening core. Cement soil mixing piles can be formed by deep mixing, powder spraying, or high-pressure rotary spraying [16]. Cement soil composite tubular pile can be divided into the short core pile, equal core pile, and long core pile according to the core pile length. They are divided into equal section piles (square, circular, annular lamp, pyramid, or combined type) and nonequal section piles (wedge and cone) according to the geometry of core piles. Among them, constant section tubular piles are more common. According to whether the peripheral surface of the core pile is regular, it can be divided into the smooth type and ribbed type [17], as shown in Figure 5:

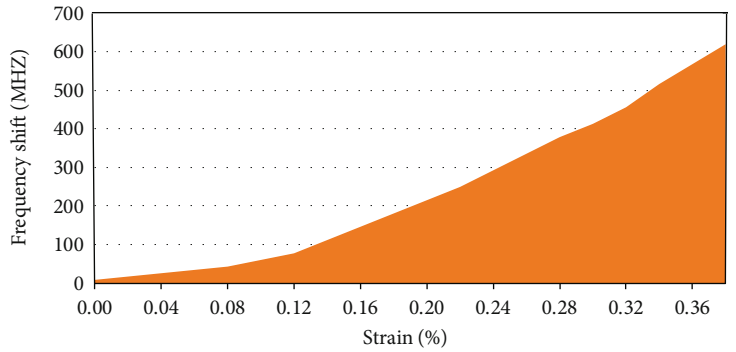

Figure 3: Relationship between Brillouin frequency shift and strain.

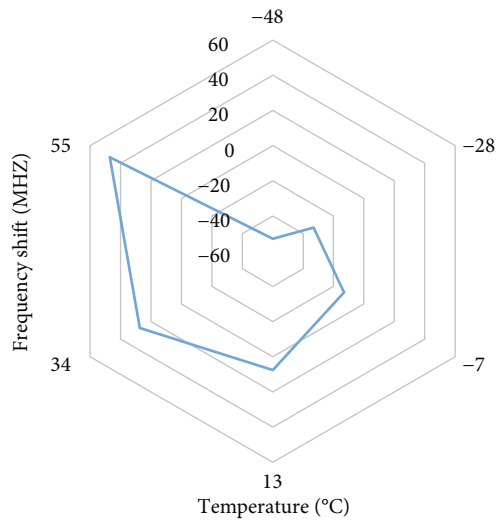

Figure 4: Relationship between Brillouin frequency shift and temperature.

2.5. Calculation of Bearing Capacity of Composite Pile. National regulations and standards: the bearing capacity of a single pile of cement soil composite pile is composed of the frictional resistance Q_{su} on the side of the composite pile and the frictional resistance Q_{pu} on the cross-section of the cement soil composite pile. When the interaction between the end face resistance and the side resistance is ignored, the bearing capacity of a single pile is [18]:

$$Q_u = Q_{su} + Q_{pu} = \sum U_i L_i q_{sui} + A_p q_{pu}. \quad (4)$$

U_i refers to the perimeter of the composite pile of the soil layer i around the pile, and L_i is the corresponding thickness of the i-th layer of soil around the pile. q_{sui} is the ultimate side friction resistance of the i-th layer of soil. q_{pu} is the end face resistance of layer i soil to the pile end.

For the loose rigid composite pile, it is generally considered that its failure surface is located in the inner and outer core sections, so its vertical resist compression bearing capacity can be estimated through Equations (5) and (6). For rigid-flexible composite pile and multielement composite pile, according to the form of failure, it can be calculated through equations (5)–(8) [19];

Long core pile:

$$R_a = u^c q_{sa}^c l^c + u^c \sum q_{sja}^c l_j + q_{pa}^c A_p^c. \quad (5)$$

Short core pile and equal core pile:

$$Ra = u^c q_{sa}^c l^c + q_{pa}^c A_p^c. \quad (6)$$

The failure surface of the side of the rigid composite pile is at the section of the composite pile core and the soil around the pile. The equations for estimating the resist compression bearing capacity of composite piles are Equation (7) and Equation (8) [20]:

Long core pile:

$$R_a = u \sum \varepsilon_{si} q_{sia} l_i + u^c \sum q_{sja} l_j + q_{pa}^c A_p^c. \quad (7)$$

Short core pile and equal core pile:

$$R_a = u \sum \xi_{si} q_{sia} l_i + \alpha \xi_p q_{pa} A_p. \quad (8)$$

R_a is the characteristic value of vertical resist compressive bearing capacity of cement soil composite pile. u^c and u are the perimeter of the inner core pile and composite section pile of cement soil composite pile, respectively. l^C is the length of the composite section of the cement soil composite pile, and l_j is the thickness of the j-th soil layer of the length of the noncomposite section. A_P^c and A_p are the area of the inner core section of the cement soil composite pile and the area of the composite section pile, respectively. q_{sa}^c is the friction resistance of the inner core side of the composite section of cement soil composite pile.

q_{sja}^c refers to the side friction of the j-th layer of the inner core of the noncomposite section of the cement soil composite pile. q_{sia} is the side friction resistance of the i-th layer of the outer core of the cement soil composite pile. q_{pa}^c and q_{pa} are the end resistance of the inner core pile end of the cement soil composite pile and the pressure of the end of

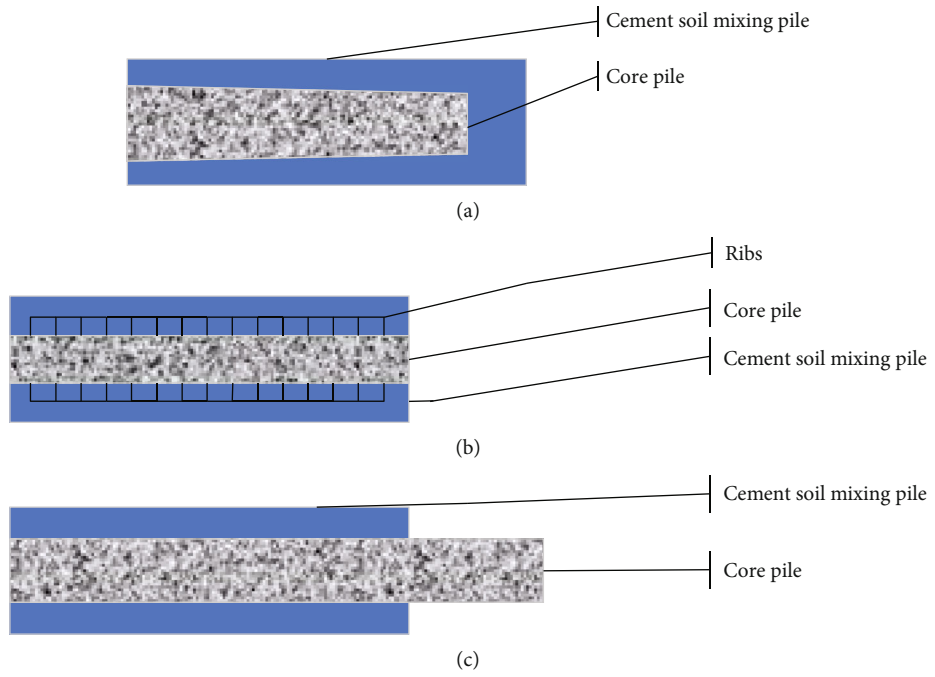

Figure 5: Types of cement soil composite tubular pile (a) short-core pile; (b) equal-core pile; (c) long-core pile.

the cement soil composite pile, respectively. There is a great relationship between the vertical bearing capacity of composite piles and the failure forms of composite piles. The failure forms of composite piles have four primary cases [21]: compression failure occurs at the upper part of tubular piles, relative sliding failure occurs at the side of cement soil piles, large sliding failure occurs between cement soil piles and tubular piles, and failure occurs when foreign matters penetrate the pile ends. Currently, the calculation equation involving long core composite piles is as follows [22].

$$R_{a1} = \xi u_p \sum_{0}^{L} q_{sia} L_i + \alpha q_p A_p + u_c \sum_{L}^{l} q_c^{sia} L_i + q_{pa}^c A_c, \quad (9)$$

$$R_{a2} = \psi_c A_c f_{ck}^c + \eta f_{cu} A_p, \quad (10)$$

$$R_{a3} = \zeta_c \eta f_{cu} A_{cf} + u_c \sum_{L}^{l} q_c^{sia} L_i + q_{pa}^c A_c, \quad (11)$$

$$R_{a3} = \xi u_p \sum_{0}^{L} q_{sia} L_i + \alpha q_{pa} A_p + \Psi A_c f_{ck}^c. \quad (12)$$

Equation (9) is to assume damage to the outer surface of cement soil. Equation (10) is to assume failure due to insufficient compressive bearing capacity of the pile body. Equation (11) is to assume failure of the inner and outer cores of cement soil. Equation (12) is to assume that the failure location is in the concrete of the noncomposite section.

2.6. New Foundation Treatment Technology Supported by Optical Fiber Sensing Technology. This exploration summarizes the worldwide research on the road problems, such as pavement subsidence and cracking in road engineering. It conducts theoretical analysis and research on engineering practice and indoor tests. The research contents are as follows:

(1) The optical fiber sensing technology is studied. The sensing parameters of temperature change and strain of optical fibers are studied by marking the temperature change and strain of optical fibers. The sensitivity of sensing fiber is compared, the factors affecting the sensitivity of optical fiber sensing are studied, and the reliability of the optical fiber sensing system is tested. Based on the principle of BOTDR, the measurement scheme of BOTDR with deformation and failure of the subgrade is designed

(2) With a road project in Hangzhou as the simulation object, a 20 : 1 road model is established indoors. According to the designed measurement scheme, the optical fiber is embedded in the road model to verify the possibility of optical fiber measuring soil and gravel settlement, and to verify the synchronous deformation ability of optical fiber and road. The measurement results of the sensing fiber are compared with that of the dial indicator, and the reliability and accuracy of the sensing fiber measuring the subgrade deformation failure are analyzed

(3) The stress of each segment of the tubular pile of cement soil composite pile under load is studied. For the bored precast pile, when making the reinforcement cage, it is essential to place the measuring stress gauge at the appropriate position and export it

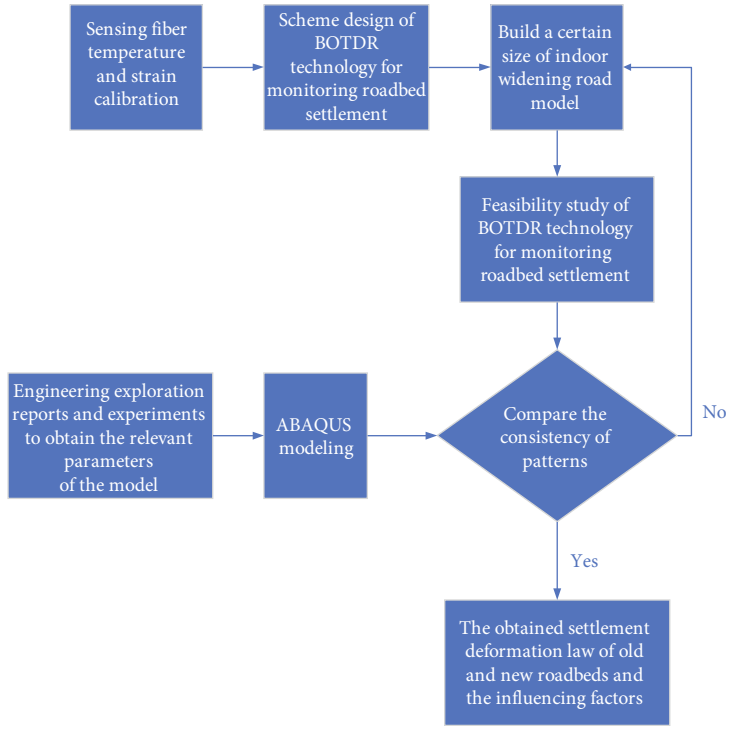

Figure 6: Technology roadmap.

along with the longitudinal reinforcement. In order to measure the axial force of the tubular pile during the tubular pile's manufacturing process, it is necessary to weld and fix the stress meter of the measuring reinforcement on the steel bar of the tubular pile

(4) In the indoor research, the dangerous simulated subgrade section is selected, and the sensing fiber and corresponding monitoring equipment are arranged to detect the settlement difference of the subgrade and the deformation and settlement of the cement soil composite tubular pile. The measured data are collected at regular intervals, and the subgrade settlement deformation measured by the sensing optical cable and the stress-strain data of the cement soil composite tubular pile are analyzed. The reliability of sensing optical cable monitoring subgrade deformation to prevent road collapse and deformation is analyzed

Based on summarizing and investigating the research on the differential settlement of new and old subgrade and worldwide BOTDR monitoring, this exploration mainly adopts the technical route of combining indoor test research, numerical analysis and comparison, engineering practice, and other means. Figure 6 displays the technical route.

Figure 6 reveals that the implementation steps of the new foundation treatment method proposed based on optical fiber sensing technology are as follows. The first step is to calibrate the optical fiber sensing temperature and strain. The second step is to use BOTDR technology to construct a monitoring scheme for subgrade settlement. The third step

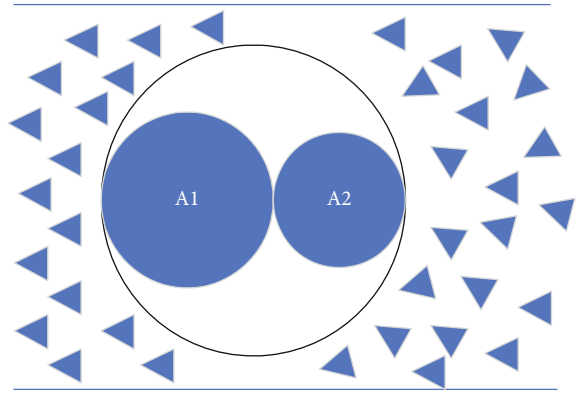

Figure 7: Schematic diagram of implantable fixed optical fiber laying.

Table 1: Parameters of measurement system.

Technical indicators	Parameters
Working temperature	5-40°C
Power supply	150-240 VAC/50-60 Hz
Sensing fiber	Standard single mode fiber
Spatial resolution	≤1.2 m
Measurement range of Brillouin frequency shift	10GHz-13GHz
Resolution of Brillouin frequency shift measurement	≤0.1 MHz

Table 2: Optical fiber information.

Fiber type	Length (m)	Diameter (mm)	Surface material	Strain sensing coefficient/(MHZ/%)	Temperature sensing coefficient/(MHZ/°C)
A1	100	3.00	Polyurethane	498	2.96
A2	100	0.8	Nylon	505	2.99

is to build a certain size indoor widening road model. The fourth step is to analyze the feasibility of the subgrade settlement monitoring method based on BOTDR technology. The fifth step is to obtain the settlement deformation law of the indoor widened road by using BOTDR technology. The sixth step is to get the model parameters according to the actual investigation. The seventh step is to use ABAQUS to model. Finally, by comparing and analyzing whether the settlement law is consistent, the deformation law of new and old subgrade settlements is obtained.

2.7. Synchronous Deformation of Optical Fiber and Subgrade. When the optical fiber is applied in subgrade engineering, optical fiber is implanted into subgrade filler. The protection of sensing fiber should be considered when using implantable methods. The sensing fiber can be directly filled into the loose soil. When the medium contains crushed stone or hard materials, these crushed stones or hard materials will cut the optical fiber and make it invalid, and the optical fiber cannot accurately reflect the subgrade condition. Hence, the surrounding medium must be treated when the implantable optical fiber is adopted in the crushed stone or hard material subgrade. Figure 7 is the schematic diagram of implantable fixed optical fiber laying:

2.8. Temperature Compensation. The temperature compensation of optical fiber has direct and indirect methods. The indirect method first measures the surrounding temperature environment, marks the temperature parameters of the optical fiber, and uses the conversion equation between temperature and Brillouin frequency shift to calculate the temperature value that needs to be compensated. The direct method is to keep the stress around the optical fiber stable, and the optical fiber is in a loose state. The temperature compensation is conducted by testing the tension state of the optical fiber through the analytical instrument. When arranging the optical fiber measurement line, an unstressed loose optical fiber needs to be arranged to compensate for the temperature of the whole optical fiber laying line. The Brillouin frequencies of the two sensing fibers are compared to obtain the optical fiber deformation frequency's change value. The indirect method first needs to mark the sensor, and then needs a thermometer to measure the temperature, and then convert it through various equations. In this way, the error is relatively large. When the measured area is relatively large, more thermometers need to be arranged, which is cumbersome to operate and inconvenient to mark the sensor. Hence, the indirect method is rarely used in engineering practice. When the onsite temperature change is less than 4°C, the influence of temperature on the frequency shift change can be ignored.

Table 3: Relationship between temperature and Brillouin frequency.

Temperature/°C	A1- Brillouin frequency/GHz	A2- Brillouin frequency/GHz
25	10.81668	10.82941
35	10.83838	10.84176
45	10.87717	10.85941
55	10.89034	10.88412
65	10.9	10.90588

2.9. Experimental Preparation. In order to verify the effect of the measurement system based on BOTDR technology, the system operation environment is first designed, then, the monitoring time of the system is set to obtain effective data, and finally the data are saved and processed. Table 1 displays the parameters of the measurement system based on BOTDR technology.

Table 1 suggests that when using BOTDR technology to measure various variables of optical fiber, high temperature may cause damage to the experimental equipment, thus affecting the measurement results. Therefore, the operating temperature is set at 5-40°C. The power supply voltage should not be too high, and it can be controlled near 200 V, so the voltage range of the power supply given in the experiment is 150-240 V. In the experiment, its numerical value is controlled within 1.2 m to avoid excessive resolution of optical fiber. Moreover, in order to make the Brillouin frequency shift measurement more effective, the Brillouin frequency shift measurement range and Brillouin frequency shift measurement resolution are set at 10GHz-13GHz and 0.1 MHz, respectively, in the experiment.

The sensitivity of optical fiber is studied. Table 2 presents the optical fiber information used in this test:

3. Results and Analysis

3.1. Indoor Temperature Mark of the Sensing Fiber. First, the known standard quantity is inputted into the sensor to be marked through experiments, and the sensor's output is detected to obtain the correlation error between the input and output of the sensor. Table 3 and Figure 8 show the change of external temperature measured by other instruments and Brillouin light frequency measured by the system:

The influence coefficients of the temperature of A1 and A2 sensing optical fibers on Brillouin frequency shift are 2.96 MHz/°C and 2.99 MHz/°C, respectively. The coefficients of the two optical fibers are basically the same. The analysis of optical fibers shows that the coefficients of A1 and A2

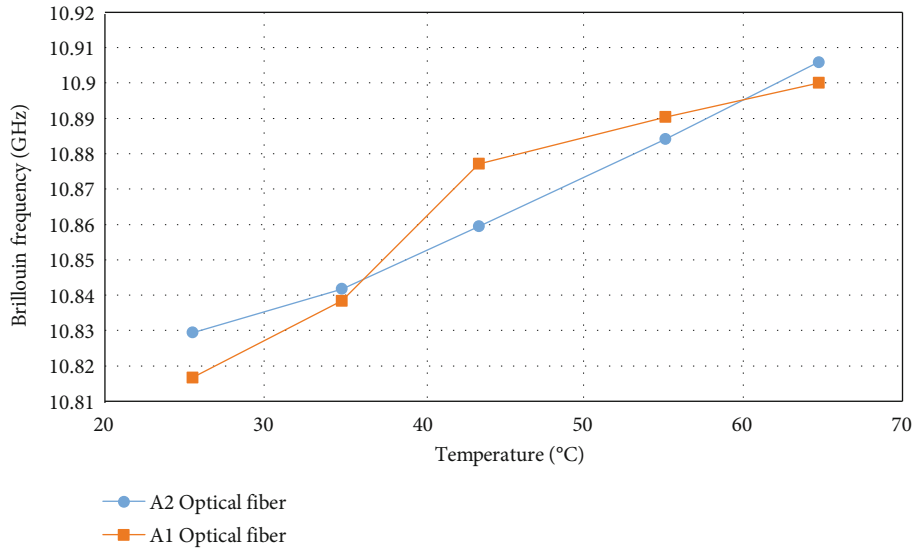

Figure 8: Relationship between temperature and Brillouin frequency.

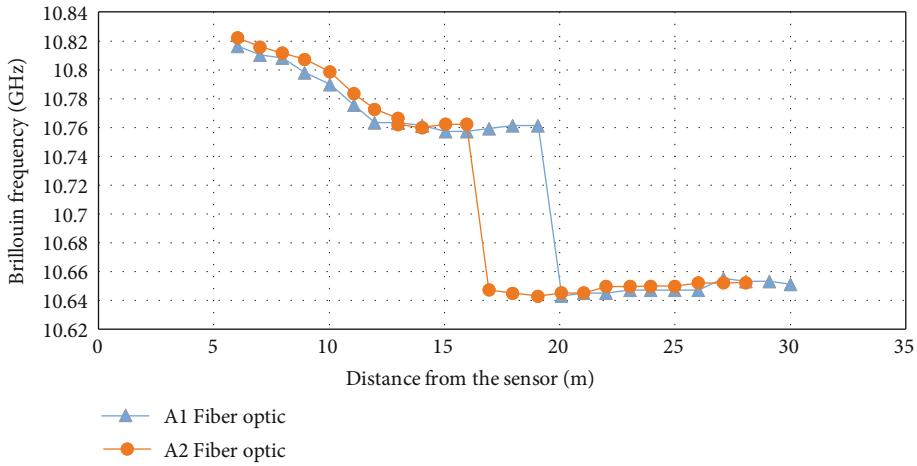

Figure 9: Monitoring results of sensing fiber on subgrade.

single-mode fibers are almost the same due to uniform heating in a constant temperature water bath. However, this does not mean that A1 and A2 sensing fibers have the same temperature sensitivity. The experimental diagram suggests that A2 fiber has a better correlation than A1 fiber, and A2 has better temperature sensitivity than A1 fiber. The diameter of A2 fiber is relatively small, so the range of acceptable temperature change is relatively large.

3.2. Feasibility Analysis of Sensing Optical Cable Project. In September 2020, the sensing fiber was placed on the monitoring section's subgrade base, the subgrade filler was backfilled, and then the mechanical compaction was conducted. In December 2020, the subgrade construction was completed, and the initial monitoring was conducted. Figure 9 displays some monitoring results:

Figure 9 suggests that the measurement functions of A1 and A2 sensing optical cables are in the normal state, and the system operates well without any abnormality. Thereby, BOTDR technology can monitor the settlement deformation of the subgrade.

3.3. Load Analysis of Cement Soil Composite Pile. The variable parameter analysis of the cement soil composite tubular pile studied in the test is conducted. For the length of the cement soil composite tubular pile, the lengths of 16 m, 18 m, 20 m, and 22 m are, respectively, taken for simulation analysis, and compared with the composite pile with the length of 24 m. Then, the composite tubular pile load with different lengths under the same vertical load is obtained. The vertical load is 5000 kN. Figure 10 displays the deformation of vertical piles with different inner core lengths:

Figure 10 suggests that the settlement effects of cement soil composite piles with different core piles under the same load are different, which indicates that the settlement degree of cement soil composite piles may be related to the core pile

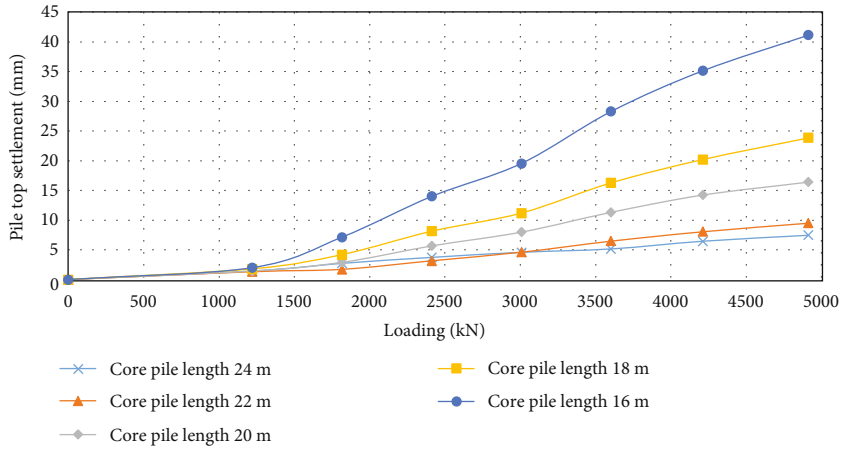

Figure 10: Deformation of vertical piles with different inner core lengths.

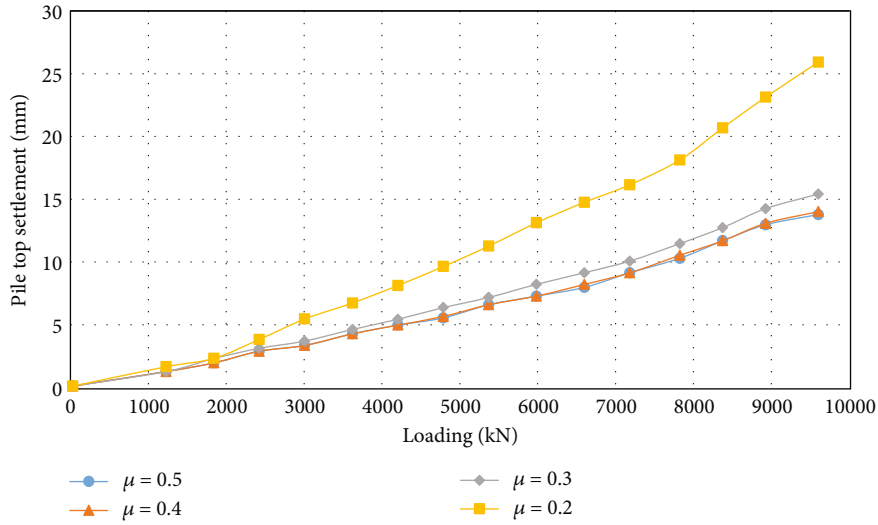

Figure 11: Influence of different friction coefficients on settlement of tubular piles.

size of composite piles. After further analysis, the relationship between the pile top settlement of the cement soil composite pile and the length of the inner core pile can be obtained. It suggests that when subjected to the same load, the longer the core pile is, the smaller the cement soil composite pile's settlement is. When the inner core pile is 20 m ~24 m long, the settlement amplitude of the cement soil composite pile is small. When the length of the inner core tubular pile is 16 m ~20 m, the settlement range of the cement soil composite pile becomes larger.

In the manufacturing process of cement soil composite tubular pile, the friction between cement soil composite tubular pile and the surrounding soil layer will be different due to the different material composition, material ratio, and manufacturing process of cement soil mixing pile. Usually, the tubular pile made by the dry method will have a large shear effect on the surrounding soil layer during the construction process to split the surrounding soil layer, and absorb the water of some surrounding soil layers, increasing the shear strength of the surrounding soil layer. On the contrary, the composite tubular pile made through the wet method increases the water content of the surrounding soil layer during the construction process, and the strength of the soil layer around the composite tubular pile will be reduced. Different soil layers will produce different friction coefficients μ for tubular piles. Figure 11 displays the influence of different friction coefficients on the settlement of tubular piles:

Figure 11 suggests that the settlement degree of the same cement soil composite pile under different friction coefficients is different. It shows that the settlement of the cement soil composite pile may be related to the friction coefficient between the pile and the soil. After further analysis, the influence of different friction coefficients on tubular pile settlement can be known. With the increase of friction coefficient, the settlement distance of tubular piles will decrease.

3.4. Relationship between Road Settlement and Cement Soil Composite Tubular Pile Settlement. Figure 12 displays the road settlement and cement soil composite tubular pile settlement:

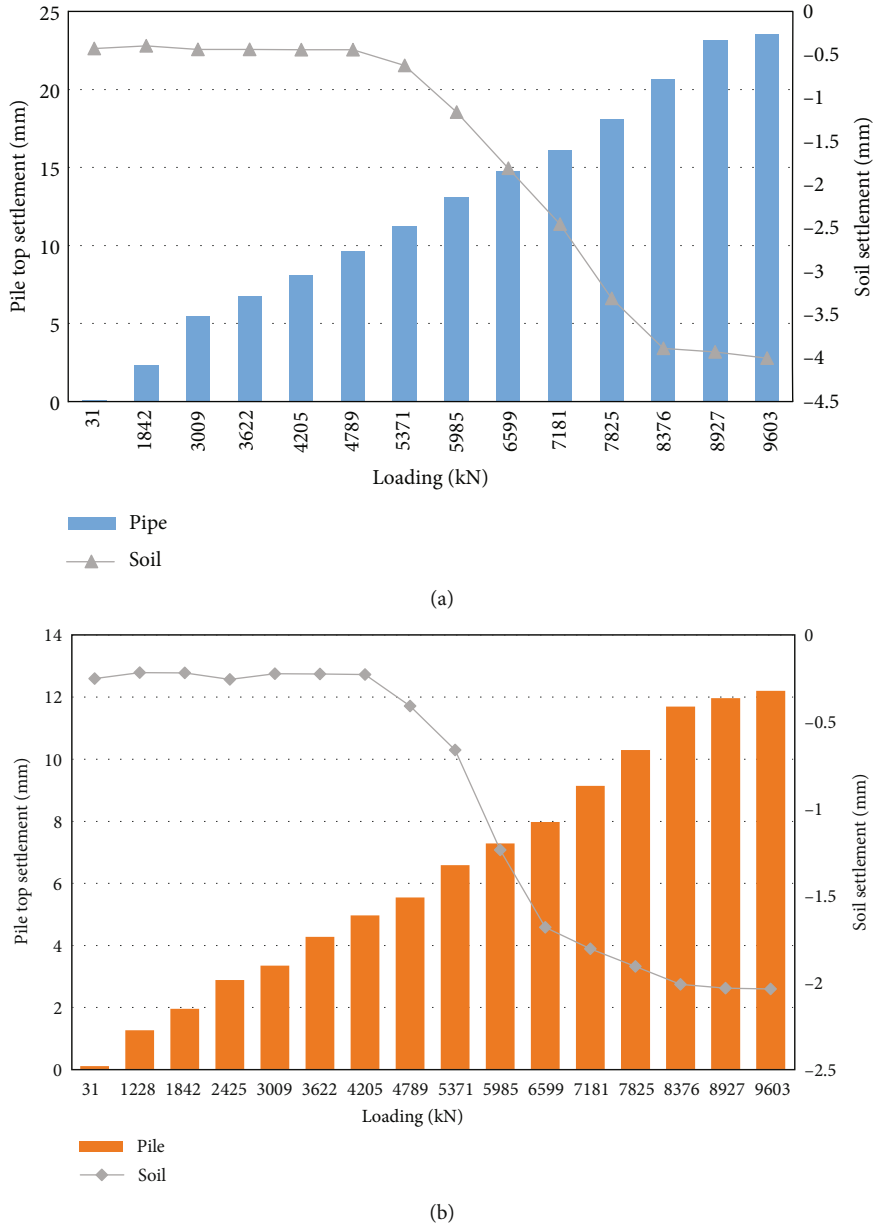

Figure 12: Road settlement and cement soil composite tubular pile settlement (a) $\mu = 0.2 \sim 0.4$; (b) $\mu = 0.4 \sim 0.5$.

Figure 12(a) reveals that when the friction coefficient μ between piles and soil is $0.2 \sim 0.4$, the pavement begins to settle under a load of 4789 kN. When the load increases to 8927 kN, the pavement settlement tends to be stable. The measured settlement of cement soil composite tubular pile is 14 mm, the settlement of pavement is 4 mm, and the settlement ratio of pavement and cement soil composite tubular pile is 28.57%. It can be considered that when the friction coefficient changes in this interval, it greatly impacts the settlement of composite piles. Figure 12(b) reveals that when μ is $0.4 \sim 0.5$, the pavement begins to settle when it is loaded with 4789 kN. When the load increases to 8376 kN, the pavement settlement tends to be stable. The measured settlement of cement tubular piles is 7 mm, the pavement settlement is 1.6 mm, and the settlement ratio of pavement to cement soil composite tubular pile is reduced by 22.86%. With the increase of pile top load, the friction between cement soil composite tubular pile and surrounding soil layer will also increase. After reaching a certain limit, this friction will remain unchanged. With the increase of the friction coefficient, the pile top load will cause the settlement of the surrounding soil layer, and the influence range of the surrounding soil layer settlement will gradually increase. However, the settlement of cement soil composite tubular piles will gradually decrease.

4. Conclusion

In recent years, optical fiber sensing technology has been widely used in foundation treatment, and has achieved good results. This exploration aims to integrate BOTDR technology with optical fiber sensing technology to achieve a better

foundation treatment effect. Hence, a new foundation treatment technology supported by optical fiber sensing technology is proposed based on the application of cement soil composite tubular pile, and its comprehensive evaluation is conducted. It is found that the application of sensing fiber to monitor the settlement of soil and gravel is feasible, and the synchronous deformation ability of the sensing fiber and subgrade is relatively good. By measuring the influence parameters of the temperature of A1 and A2 sensing fibers on Brillouin frequency shift, it is found that the diameter, sheath thickness, and type of sensing fibers impact the temperature sensing coefficient and strain sensing coefficient. The settlement of composite piles decreases with the increase of tubular pile length. When the friction coefficient μ between the pile-soil interface changes between $0.2 \sim 0.4$, the settlement of composite piles varies widely. When μ changes between $0.4 \sim 0.5$, the variation range of composite pile settlement is small. The relationship between the settlement of cement soil composite tubular pile and subgrade settlement is measured under different friction coefficients between pile and soil interface. With the load increase, the settlement of cement soil composite tubular pile in the pile-soil layer with a small friction coefficient is greater than that of the tubular pile in the pile-soil layer with a large friction coefficient. Moreover, the friction coefficient's inconsistency also affects the pavement settlement. The pavement settlement with a large friction coefficient between pile and soil interface is also smaller than that of pavement with a small friction coefficient. The purpose is to further optimize the optical fiber sensing technology by using BOTDR technology to better apply it to the foundation treatment work, and obtain a higher quality foundation treatment effect.

Due to the limited time, the monitoring time for the foundation settlement deformation law and the cement soil composite tubular pile's settlement law is relatively short. Hence, the complete monitoring data of sensing optical cables and conventional monitoring instruments in the project cannot be obtained. Long-term observation will be conducted in future research to verify the accuracy of the application of sensing optical cables in civil engineering.

Data Availability

The data used to support the findings of this study are available from the corresponding author upon request.

Conflicts of Interest

The author declares that there are no known competing financial interests.

Acknowledgments

This work was supported by the Key Project of Natural Science Foundation of Zhejiang Province (grant no. LXZ22E080001) and National Natural Science Foundation of China (grant nos. 52178358 and 52108349).

References

[1] X. Wang, X. Cao, H. Xu et al., "Research on the properties of peat soil and foundation treatment technology," *E3S Web of Conferences*, vol. 272, article 02019, 2021.

[2] L. Shao, Q. Wang, G. Qin, and R. Liu, "Elementary discussion on construction technology of foundation treatment for water conservancy and hydropower projects," *Smart Construction Research*, vol. 2, no. 3, 2018.

[3] X. C. Lao and X. F. Zhang, "Reinforcement scheme and construction technology for leakage treatment sof deep well foundation pit," *Guabfzhou Architecture*, vol. 49, no. 3, p. 33, 2021.

[4] J. Li, D. Zheng, L. Wu, and F. Wang, "Application of visualization modeling technology in the determination of reinforcement range of deep soft soil foundation," *Environmental Earth Sciences*, vol. 81, no. 7, pp. 1–13, 2022.

[5] N. Lalam, W. P. Ng, X. Dai, Q. Wu, and Y. Q. Fu, "Performance improvement of Brillouin ring laser based BOTDR system employing a wavelength diversity technique," *Journal of Lightwave Technology*, vol. 36, no. 4, pp. 1084–1090, 2018.

[6] D. Tosi, E. Schena, C. Molardi, and S. Korganbayev, "Fiber optic sensors for sub-centimeter spatially resolved measurements: review and biomedical applications," *Optical Fiber Technology*, vol. 43, pp. 6–19, 2018.

[7] H. D. Bhatta, L. Costa, A. Garcia-Ruiz et al., "Dynamic measurements of 1000 microstrains using chirped-pulse phase-sensitive optical time-domain reflectometry," *Journal of Lightwave Technology*, vol. 37, no. 18, pp. 4888–4895, 2019.

[8] G. Bashan, H. H. Diamandi, Y. London, E. Preter, and A. Zadok, "Optomechanical time-domain reflectometry," *Nature Communications*, vol. 9, no. 1, pp. 1–9, 2018.

[9] A. Aitkulov and D. Tosi, "Optical fiber sensor based on plastic optical fiber and smartphone for measurement of the breathing rate," *IEEE Sensors Journal*, vol. 19, no. 9, pp. 3282–3287, 2019.

[10] M. Shanafield, E. W. Banks, J. W. Arkwright, and M. B. Hausner, "Fiber-optic sensing for environmental applications: where we have come from and what is possible," *Water Resources Research*, vol. 54, no. 11, pp. 8552–8557, 2018.

[11] F. L. Barkov, Y. A. Konstantinov, and A. I. Krivosheev, "A novel method of spectra processing for brillouin optical time domain reflectometry," *Fibers*, vol. 8, no. 9, p. 60, 2020.

[12] A. Zafeiropoulou, A. Masoudi, A. Zdagkas, L. Cooper, and G. Brambilla, "Curvature sensing with a D-shaped multicore fibre and Brillouin optical time-domain reflectometry," *Optics Express*, vol. 28, no. 2, pp. 1291–1299, 2020.

[13] T. Horiguchi, Y. Masui, and M. S. D. Zan, "Analysis of phase-shift pulse brillouin optical time-domain reflectometry," *Sensors*, vol. 19, no. 7, p. 1497, 2019.

[14] S. K. Almoosa, A. E. Hamzah, M. S. D. Zan, M. F. Ibrahim, N. Arsad, and M. M. Elgaud, "Improving the Brillouin frequency shift measurement resolution in the Brillouin optical time domain reflectometry (BOTDR) fiber sensor by artificial neural network (ANN)," *Optical Fiber Technology*, vol. 70, p. 102860, 2022.

[15] T. Oda, A. Nakamura, Y. Koshikiya, and N. Honda, "Brillouin optical time domain reflectometry for estimating loss and crosstalk at the splice point in few-mode fibers," *Optical Fiber Technology*, vol. 68, article 102741, 2022.

[16] S. Yang, M. Zhang, X. Bai, X. Liu, and C. Zheng, "Experiment investigation on stress characteristics of grouting microsteel

pipe piles with cement-soil wall," *Advances in Materials Science and Engineering*, vol. 2020, Article ID 9704589, 10 pages, 2020.

[17] X. Lu, M. Song, and P. Wang, "Numerical simulation of the composite foundation of cement soil mixing piles using FLAC3D," *Cluster Computing*, vol. 22, no. S4, pp. 7965–7974, 2019.

[18] Y. Wu, K. Zhang, L. Fu, J. Liu, and J. He, "Performance of cement–soil pile composite foundation with lateral constraint," *Arabian Journal for Science and Engineering*, vol. 44, no. 5, pp. 4693–4702, 2019.

[19] R. Liu and C. Liang, "Study of the bearing capacity at the variable cross-section of a riser-surface casing composite pile," *China Ocean Engineering*, vol. 35, no. 2, pp. 262–271, 2021.

[20] X. Wang, Y. Que, K. Wang et al., "Modeling test and numerical simulation of vertical bearing performance for rigid-flexible composite pouch piles with expanded bottom (RFCPPEB)," *Symmetry*, vol. 14, no. 1, p. 107, 2022.

[21] N. B. Umravia and C. H. Solanki, "Comparative study of existing cement fly ash gravel pile and encased stone column composite foundation," *IOP Conference Series: Materials Science and Engineering*, vol. 1197, no. 1, article 012002, 2021.

[22] C. Phutthananon, P. Jongpradist, and P. Jamsawang, "Influence of cap size and strength on settlements of TDM-piled embankments over soft ground," *Marine Georesources & Geotechnology*, vol. 38, no. 6, pp. 686–705, 2020.